PREPARATION AND CHARACTERIZATION OF HYBRID NANOMATERIALS CONTAINING MAGNETIC FE_3O_4 NANOPARTICLES AS DRUG DELIVERY SYSTEM

ŞEYMA TUNA,[*] ASLI BEYLER-ÇIĞIL[**] and SERAP DEMIR[*]

[*]*Marmara University, Faculty of Arts and Sciences, Department of Chemistry, Istanbul, Turkey*
[**]*Amasya University Technical Sciences Vocational, Department of Chemistry and Chemical Process Technology School, Amasya, Turkey*
✉ *Corresponding author: A. Beyler-Çiğil, asliibeyler@gmail.com*

Received April 28, 2022

In this study, magnetic Fe_3O_4 nanoparticles were synthesized and the magnetic surfaces of the nanoparticles were modified with thiol groups. The chitosan polymer was modified with allyl groups and then bound to magnetic nanoparticles by the thiol-en click reaction. The drugs paclitaxel (PTX) and doxorubicin (DOX) were loaded separately and together into this prepared hybrid material, and then drug releases from the hybrid material were studied. The aim of this paper is to present the results on the controlled release of DOX and PPT cancer drugs from chitosan-Fe_3O_4 nanoparticles at two different pH values (5.0 and 7.4). PTX was effectively loaded into chitosan-Fe_3O_4 nanoparticles and slowly released up to 72.66% at pH 5 and 41.45% at pH 7.4 after 48 hours. DOX was effectively loaded into chitosan-Fe_3O_4 nanoparticles and slowly released up to 30.5% at pH 5 and 23.3% at pH 7.4 after 48 hours.

Keywords: drug release, cancer drug, chitosan, thiol-en click, magnetic nanoparticles

INTRODUCTION

Cancer, one of the primary public health problems, is a malignant disease that can multiply indefinitely and affects human health, destroying the surrounding normal tissues. Although chemotherapy is a very effective treatment for primary and metastatic cancer, it has several limitations in treating cancer, including poor selectivity, high cost, and strong drug resistance.[1] In addition, in direct drug therapy, the drug is rapidly distributed in the body and peaks. Since only a little of the drug can reach the tumor site, the continuous re-administration of drugs and the increase in administration times cause undesirable results. Therefore, drug delivery systems are a good approach to increase the therapeutic effectiveness of traditional anticancer drugs.[2] The use of a single chemotherapeutic agent in conventional cancer chemotherapy may lead to failure of chemotherapy by revealing disadvantages such as toxicity, low anticancer efficacy, possible cancer cell survival, especially dose-limiting.[3] Therefore, a combined strategy of two or more therapeutic tools and different therapies is proposed as a potential way to resolve this blockage.

There are more than 70 types of drugs used for cancer treatment. Paclitaxel (PTX) and doxorubicin (DOX), used in combination with other therapies to treat a variety of neoplasms, are among the most potent anticancer drugs.[4] Paclitaxel (PTX) represents a potent and rapid inhibitor against a variety of tumor cells, including breast cancer, ovarian cancer, lung cancer, head and neck carcinomas, and acute leukemia.[5] DOX is used as an antineoplastic agent, especially to treat fluid and solid cancer, such as leukemia and breast cancer.[6] However, both drugs have disadvantages, such as neurotoxicity for PTX and dose-dependent cardiotoxicity for DOX, as well as poor pharmacokinetic properties. In addition, these two drugs differ in their physicochemical properties, pharmacokinetics and mechanisms of action, as

well as toxicity and drug resistance. Therefore, it is necessary to deliver the two drugs in full, using a highly effective and low-toxicity formulation.

Nanotechnology and combination therapy are promising areas in cancer treatment. The use of polymers as targetable drug carriers helps to improve the therapeutic efficacy of the drug while improving their pharmacokinetics, reducing the side effects associated with high dosage.[4]

In recent years, the importance of magnetic nanoparticles (MNPs) in the scientific and technological field has greatly increased. The main reason for this is the presence of magnetic nanoparticles in many fields, from single component nanoparticles to multifunctional nanocomposites that open up a wide range of applications.[7-10] Magnetic (Fe_3O_4) nanomaterials have attracted attention for drug release systems due to their superparamagnetic properties.[11] Although the magnetic part of the magnetic nanoparticles used in drug release systems consists of Fe^{+2} and Fe^{+3} salts, different polymers are used for the polymeric matrix part. For example, albumin alginate, poly(caprolactone), poly(ethylene oxide) and chitosan are the most commonly used polymeric structures.[12]

Biopolymer materials are natural substances and they adapt to the organism in studies of living organisms. Therefore, they are used in gene engineering as a holder-skeleton in cell growth experiments and in drug loading and release systems.[13] Chitosan, a polysaccharide of biological origin, attracts great interest in various fields, such as food technology, biomedical and pharmaceutical industries, due to its properties such as biodegradability, stability, high biocompatibility and low toxicity.[14]

Magnetic Fe_3O_4 nanoparticles were synthesized and the magnetic surfaces of the nanoparticles were modified with the thiol group. Then, chitosan polymer modified with allyl group was prepared and bound to magnetic nanoparticles by the click reaction. PTX and DOX were loaded on this hybrid material separately and together, and then drug release from the hybrid material was examined. Structure characterization for all steps of surface modification of Fe_3O_4 was done with ATR-FTIR and XPS. At the same time, size measurements of magnetic nanoparticles, thiol modified magnetic nanoparticles and polymer bonded magnetic nanoparticles were performed with a Zetasizer. Structure characterizations of allyl modified polymers were carried out by ATR-FTIR and ^{1}H-NMR. TGA analysis was used for examining the thermal resistance and percentage modification of the hybrid nanomaterial.

EXPERIMENTAL

Materials

Iron (II) sulfate heptahydrate ($FeSO_4.7H_2O$), iron (III) chloride ($FeCl_3$), (3-mercaptopropyl) trimethoxysilane ($HS(CH_2)_3Si(OCH_3)_3$, allyl glycidyl ether ($C_6H_{10}O_2$), chitosan, paclitaxel, doxorubicin, ammonia, ethyl alcohol, acetone and acetic acid were purchased from Sigma-Aldrich (Germany).

Preparation of Fe_3O_4 magnetic nanoparticles

Very different methods are reported in the literature for the synthesis of Fe_3O_4 nanoparticles.[15,16] Among these methods, co-precipitation is one of the most frequently used ones. For this purpose, 2.78 grams of $FeSO_4.7H_2O$ and 3.2 grams of $FeCl_3$ were transferred to a 250 mL flask and 100 mL of deionized water was added to the mixture to dissolve the two substances. The resulting mixture was kept in the reflux system for 15 minutes in N_2 gas environment at room temperature. After the ambient temperature increased from room temperature to 90 °C, 10 mL of NH_3 was added to the mixture in the reflux system and N_2 gas was passed through the environment for 2 hours. At the end of the period, the mixture was allowed to cool to room temperature and synthesized Fe_3O_4 nanoparticles were passed through a black band filter paper. After washing twice with deionized water and twice with ethanol, Fe_3O_4 nanoparticles were left to dry in a vacuum oven at 60 °C for 24 hours.

Modification of Fe_3O_4 nanoparticles

30 mL of ethanol and 20 mL of deionized water were added to 2 grams of Fe_3O_4 nanoparticles. The mixture was sonicated for 15 minutes, so that the nanoparticles dispersed homogeneously. At the end of the period, 9 drops of NH_3 and 3 mL of 3-mercaptopropyltrimethoxysilane were added to the mixture and it was sonicated for 2 hours to achieve homogeneous dispersion. At the end of the period, homogeneously dispersed nanoparticles were passed through a black band filter paper. They were washed twice in ethanol and centrifuged. The solid part remaining in the centrifuge tube was collected with a vortex device. The precipitate was left to dry at 60 °C for 24 hours. The modification process is illustrated in Figure 1.

Modification of chitosan

The modification of chitosan allyl end groups was adapted from similar studies in the literature.[17] An amount of 5 grams of chitosan was dissolved in 50 mL of 1% acetic acid-water solution. The pH of the mixture was adjusted to 8. Then, 6.962 grams of allyl glycidyl ether was added to the mixture obtained and

kept at 30 °C in a shaking water bath for three nights. Subsequently, the prepared mixture was precipitated in 150 mL of acetone and the polymer was observed to precipitate in fiber form. After the precipitation process, the allyl group modified chitosan was washed several times with acetone and ethanol and left to dry in a vacuum oven at 40 °C for 24 hours. The modification is presented in Figure 2.

Preparation of drug delivery system

An amount of 0.6 grams of thiol end group Fe_3O_4 (SH-Fe_3O_4) nanoparticles was added to 50 mL of deionized water and homogeneously dispersed in an ultrasonic bath for 2 hours and 40 minutes. 1.8 grams of chitosan-allyl was dissolved in a 1% acetic acid-water solution at 60 °C. Then, chitosan-allyl and Fe_3O_4 with thiol end groups were mixed and 6 drops of photoinitiator were added to this mixture and left in the photo-reactor for 30 minutes. At the end of the process, chitosan-Fe_3O_4 samples were passed through black band filter paper. The solid part was washed twice with deionized water, transferred to a Petri dish, covered with aluminum foil and left to dry at 60 °C in a vacuum oven. After drying, the chitosan-Fe_3O_4 nanoparticles were washed twice with deionized water and left to dry.[18] The representation of the magnetic nanoparticles prepared for the drug system is given in Figure 3.

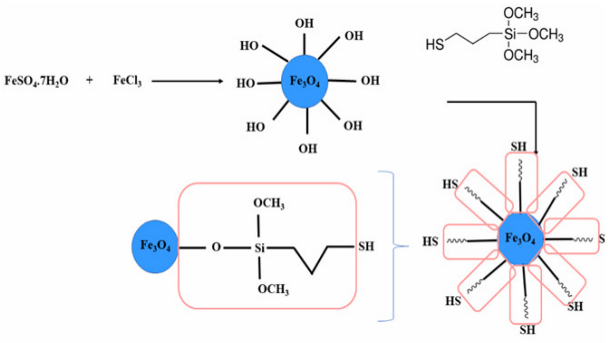

Figure 1: Schematic representation of the synthesis of magnetic nanoparticles and chemical modification with 3-mercaptopropyltrimethoxysilane

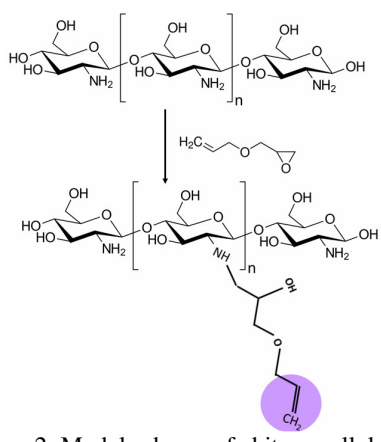

Figure 2: Model scheme of chitosan allylation

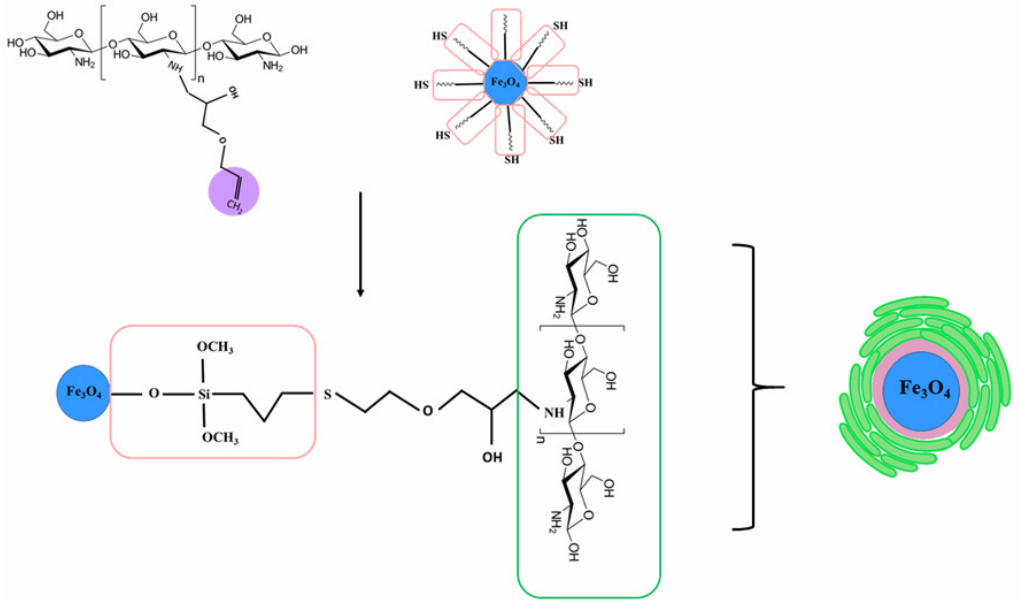

Figure 3: Chitosan-coated magnetic nanoparticles prepared for use in the drug system

Characterization methods

Attenuated total reflection Fourier transform infrared spectroscopy (ATR-FTIR): functional group analyses of Fe_3O_4 nanoparticles with thiol end groups, synthesized Fe_3O_4 nanoparticles, chitosan natural polymer and chitosan with allyl end groups were performed with a Spectrum 100 FTIR spectrophotometer device of Perkin-Elmer company. Spectra were recorded in the wavelength range of 380-4000 cm^{-1}.

Nuclear magnetic resonance (^{1}H-NMR) spectra of initial chitosan and chitosan with allyl end groups were recorded on a Bruker Advance 500 MHz spectrophotometer. Both initial and modified chitosan were dissolved in 1% acetic acid-water solution before analysis.

Thermogravimetric analysis (TGA): a Perkin Elmer Pyris 1 model TGA device was used to measure the thermo-oxidative stability of the prepared thiol modified magnetic nanoparticles. Measurements were made in air and in nitrogen atmosphere, with a heating rate of 10 °C/min, at temperatures between 30 °C-750 °C.

Scanning transmission electron microscopy (STEM): the synthesized thiol modified magnetic nanoparticles and the prepared drug transport system were gold coated and morphological investigations were made with a Phillips XL 30 ESEM-FEG/EDAX model device.

Dynamic light scattering (DLS): the size analysis of the obtained thiol modified magnetic nanoparticles and the prepared drug transport system were performed with a Brookhaven 90 Plus Nano Particle Size/Zeta Potential Analyzer. Measurements were made with a very powerful 35 mW laser, by the laser dynamic beam scattering technique (DLS), for suspended particles in the range of 2 nm-3 microns.

Zeta potential analyzer: the ζ potentials of the 2.5% (w/v) aqueous dispersions of the prepared nanoparticles were measured at room temperature by adjusting the pH of the environment in the range of pH 2.0-9.5 with HCl or NaOH.

Drug loading

An amount of 300 µg of DOX dissolved in 2 mL of distilled water was added onto 0.01 g chitosan-Fe_3O_4 nanoparticles, and kept in the dark under stirring at 200 rpm in a water bath set at 37 °C for 24 hours. The DOX loaded chitosan-Fe_3O_4 nanoparticles were separated by magnetism, washed and dried. The nanoparticles were stored in a refrigerator for characterization and drug release. The loaded drug was calculated by reading the supernatant absorbance at 480 nm recorded by the spectrophotometer. 300 µg of PTX was dissolved in 2 mL of acetonitrile and added on 0.01 g of chitosan-Fe_3O_4 nanoparticles and kept in a 37 °C water bath at 200 rpm for 24 hours. The chitosan-Fe_3O_4 nanoparticles loaded with PTX were magnetically removed, washed and dried. The remaining supernatant absorbance was read at 227 nm. The same procedure was performed to load DOX and PTX together as described above. The drug loading content (DL %) and encapsulation efficiency (EE %) were calculated by the following equations:

$$DL\ \% = (Wadded\ drug - Wfree\ drug)Wnp \times 100$$

$$EE\ \% = (Wadded\ drug - Wfree\ drug)Wadded\ drug \times 100$$

Drug release

Drug release studies were carried out in 10 mM pH 7.4 and pH 5 phosphate buffer systems. First, the drug loaded chitosan-Fe_3O_4 nanoparticles were weighed and placed into tubes; 3 mL of 10 mM pH 7.4 phosphate buffer was added and allowed to mix at 200 rpm in a water bath set at 37 °C. At various time intervals, 800 µL of sample was drawn from the media to monitor drug release using the spectrophotometer, and an equal volume of phosphate buffer was added to the dissolution medium to maintain a constant volume. The amount of drug released was calculated from the standard graphs drawn for both drugs using drug concentrations prepared in 10 mM pH 7.4 phosphate buffer. Drug release studies were repeated using 10 mM pH 5 phosphate buffer. The amounts of drug released were calculated from the standard plot obtained from drug solutions prepared using 10 mM pH 5 phosphate buffer. Each assay was carried out in triplicate.

RESULTS AND DISCUSSION

ATR-FTIR spectra

The ATR-FTIR spectra of Fe_3O_4 nanoparticles, magnetic nanoparticles after thiol modification, initial chitosan and chitosan after allyl modification are given in Figure 4 and Figure 5. A wide peak is seen in the spectra of Fe_3O_4 and Fe_3O_4-SH nanoparticles at 586 cm^{-1}. This peak is due to the characteristic Fe-O stress vibration in magnetic nanoparticles.[19,20] As seen in Figure 4, the peak at 3400 cm^{-1} is caused by the -OH stretching vibration in Fe_3O_4 nanoparticles.[21] When the spectrum of Fe_3O_4-SH is examined, the peak of C-S stretch vibration is seen at 686 cm^{-1}, which is different from that of Fe_3O_4 nanoparticles.[22] It can also be attributed to the stress vibration of the peak S-H at 2570-2590 cm^{-1}, but the S-H stretch vibration is generally not very clear.[21] However, the peak at 2850-2900 cm^{-1} is due to the C-H stretching vibration of the methylene group at 3-mercaptopropyltrimethoxysilane. In addition, the Si-O bending vibration peak of the silanol group is seen at 964 cm^{-1}.[22] In the literature, similar peaks were observed in ATR-FTIR spectra, which

were obtained as a result of the reaction with 3-mercaptopropyltrimethoxysilane after Fe_3O_4 nanoparticles were first coated with SiO_2.[20] When the results are examined and compared with the literature, it is seen that the surface modification of Fe_3O_4 nanoparticles with thiol end groups has been successfully performed.

Figure 5 shows the ATR-FTIR spectra of chitosan with allyl glycidyl ether, initial chitosan and allyl end groups. The allyl groups were attached to the chitosan skeleton by the epoxy-amine reaction. Looking at the spectrum of chitosan, the stress vibration of the strong and broadband O-H and N-H bonds is noted at 3200-3500 cm^{-1}. The peak corresponding to the stretching of the C-H bond is seen at 2910 cm^{-1}. Apart from these, the stress vibration of the C-O-C bonds of the polysaccharide skeleton is seen at 1028 cm^{-1}, and the characteristic peaks of the-1,4-glycosidic bond – at 1153 and 895 cm^{-1}. Apart from all these peaks, the peak seen at 1595 cm^{-1} corresponds to the N-H vibration of the primary amine.[17,23] In the spectrum of chitosan modified by the reaction with allyl glycidyl ether, the peak of the primary amine at 1590 cm^{-1} is less intense than that of unmodified chitosan. Allyl bands are difficult to characterize because of the overlap with other peaks, as well as a limited functionalization rate.[14]

^{1}H-NMR spectra

After the reaction of chitosan and allyl glycidyl ether, ^{1}H-NMR spectra were taken to confirm the synthesis of the desired chitosan-allyl compound and the resulting signals were examined.

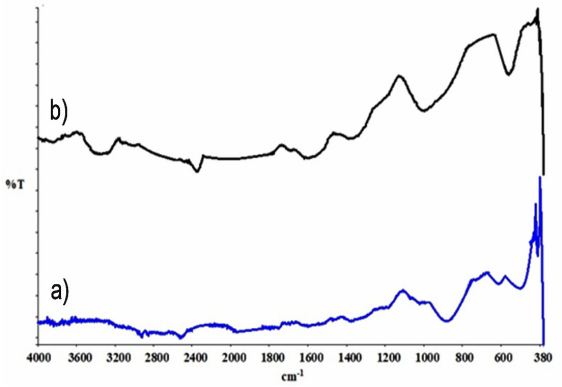

Figure 4: ATR-FTIR spectra of a) pure Fe_3O_4 nanoparticles and b) Fe_3O_4 nanoparticles modified by 3-mercaptopropyltrimethoxysilane

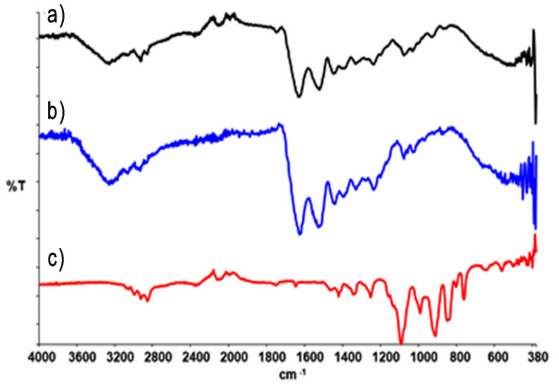

Figure 5: ATR-FTIR spectra of a) chitosan-allyl, b) initial chitosan and c) allyl glycidyl ether

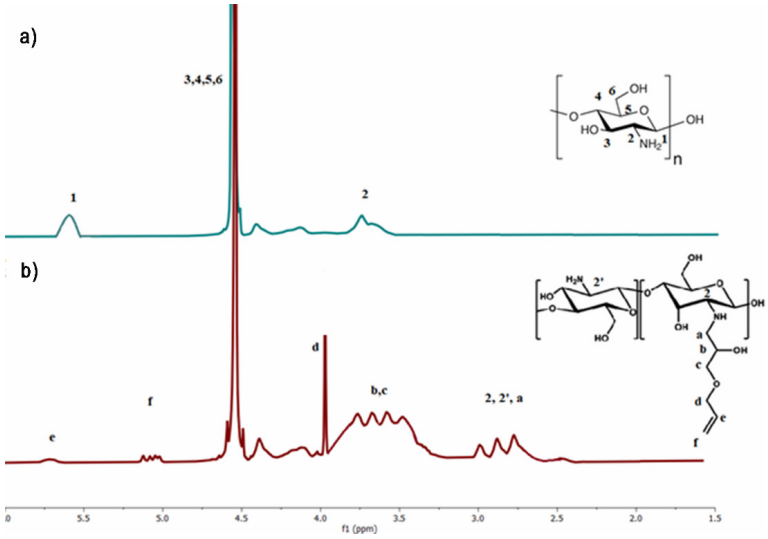

Figure 6: ^{1}H-NMR spectra of a) initial chitosan and b) chitosan-allyl

The ^{1}H-NMR spectra of initial chitosan and chitosan-allyl are shown in Figure 6. The proton signals for chitosan appeared as follows: hydrogen signal (H_1) attached to the anomeric carbon $5.3 < \delta < 5.5$ ppm and hydrogens attached to the third, fourth, fifth and sixth carbon in glucosamine units (H_3, H_4, H_5, H_6) $4 < \delta < 4.9$ ppm. Also, the signal of hydrogen bound to the second carbon in the glucosamine unit is seen at 3.7 ppm. When compared with the ^{1}H-NMR spectra previously taken for chitosan, it was found to be compatible with the literature.[18] New signals, due to allyl glycidyl ether, are seen in the spectrum of chitosan modified with allyl end group: 5.84-6.20 ppm ($CH_2 = CHCH_2O$), 5.23-5.34 ppm ($CH_2 = CHCH_2O$) and 4.01-4.16 ($CH_2 = CHCH_2O$). The results were found to be compatible with those reported in the literature.[17]

Particle size distribution and zeta potential

Size distributions of synthesized Fe_3O_4 nanoparticles, magnetic nanoparticles modified with thiol end groups and chitosan coated magnetic nanoparticles are shown in Figure 7. The approximate mean diameter of Fe_3O_4 nanoparticles was measured as 46 nm. In a study reported in the literature, the dimensions of spherical magnetic nanoparticles obtained by the co-precipitation method were measured as 30-100 nm.[24-26] In another study, the authors found that 80% of the magnetic nanoparticles prepared by the co-precipitation procedure consisted of 30-55 nm size nanoparticles. Comparing these results, it can be concluded that the magnetic nanoparticles prepared in the present study are compatible in terms of diameter with those reported in the literature. However, after the treatment with 3-mercaptopropyltrimethoxysilane, the size of Fe_3O_4 nanoparticles increased noticeably (Fig. 7b). The mean diameter of Fe_3O_4-SH nanoparticles was measured as 82 nm. This increase indicates that the addition of organosilane leads to an increase in the size of the nucleus.[27] In the literature, researchers reported that the size of magnetic nanoparticles, initially smaller than 100 nm, increased to approximately 600 nm after coating with 3-mercaptopropyltrimethoxysilane.[28] In another study conducted in 2014, it was reported that the size of magnetic nanoparticles measured approximately 8 nm by TEM analysis increased to 10 nm after coating with 16-mercaptohexadecanoic acid.[29,30] The size increase in Fe_3O_4-SH nanoparticles, compared to magnetic nanoparticles, is an expected situation, as confirmed by other studies in the literature.

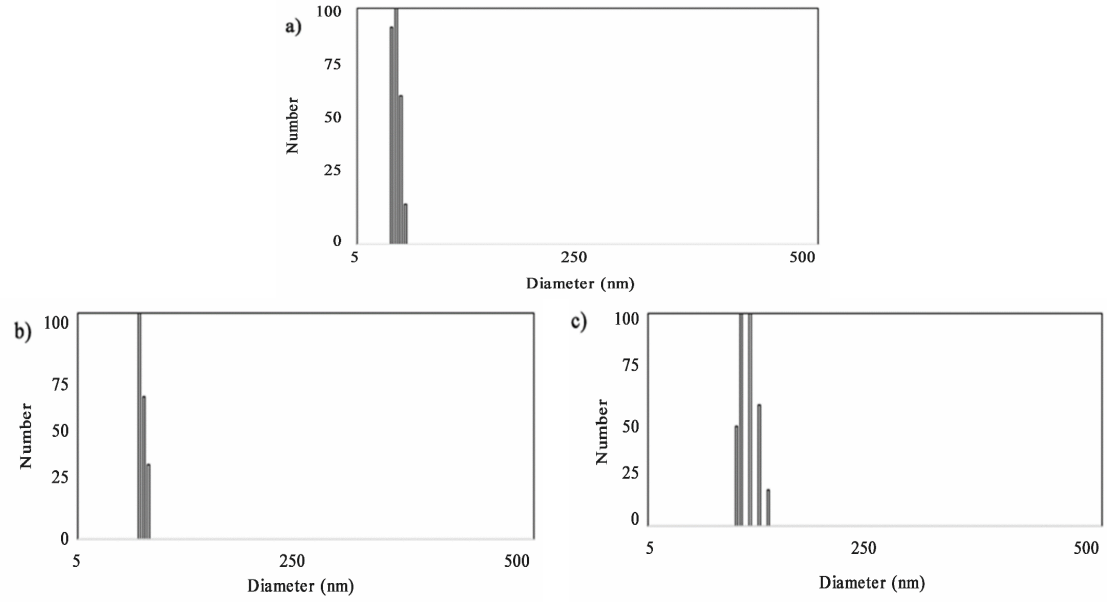

Figure 7: Size distribution of a) Fe_3O_4 nanoparticles, b) Fe_3O_4-SH nanoparticles and c) chitosan coated magnetic nanoparticles

It is seen in Figure 7c that the size of the chitosan coated magnetic nanoparticles increases even more. Its approximate hydrodynamic dimension was measured as 142 nm. In the literature, when the size of magnetic nanoparticles synthesized for biocompatibility studies is measured by dynamic

light scattering (DLS), the largest percentage of dispersion is 18 nm, while this value is 35 nm for chitosan-coated iron oxide nanoparticles.[31] Generally, the hydrodynamic size achieved with DLS in aqueous suspension is large due to the thickness of the solvation layer and nanoparticle aggregation. However, as a drug carrier, the desired size distribution of the particles ranges from 10 nm to 200 nm,[32] so the sizes of chitosan-coated magnetic nanoparticles belong to an appropriate scale for drug carrier application. In a previous study, in the DLS analysis of Fe_3O_4 magnetic nanoparticles modified with chitosan cross-linked carboxymethyl-cyclodextrin polymer prepared for hydrophobic drug release, the average dimensions were given as 67-78 nm.[32] In the light of all these data, it can be established that the size of the prepared magnetic nanoparticles is compatible with the literature and suitable for drug release.

Table 1
Zeta potential values of prepared nanoparticles

Sample	Zeta potential, mV
Fe_3O_4 nanoparticles	-17.6
Fe_3O_4-SH nanoparticles	-23.4
Chitosan coated magnetic nanoparticles	-27.8

Due to chitosan or 3-mercaptopropyltrimethoxysilane conjugation and charge on the surface of the nanoparticles, the tight binding leads to intense repulsion among the nanoparticles and maintains the stability of the nanoparticle suspension. Therefore, the zeta-potential measurement is considered an important parameter to provide evidence for the charge of the nanoparticles obtained. The surface charges and surface chemistry of the obtained nanoparticles change depending on the various functional groups bound on the Fe_3O_4 surface at different modification stages. As given in Table 1, the negative zeta potential (ζ) value of Fe_3O_4 nanoparticles of -17.6 mV (at pH 7.0) can be attributed to the presence of hydroxyl groups on the surface under basic synthesis conditions. After modification with 3-mercaptopropyl trimethoxysilane, the value of zeta potential decreases to -23.4 mV, because of the presence of thiol groups on the surface. After coating with chitosan, the value of nanoparticles decreases to -27.8 mV, owing to the presence of excessive amounts of carboxymethyl groups; carboxylic acid groups are responsible for negative charges. This important difference in surface electrokinetics indicates that the zeta potential depends on the shell properties. These results show that 3-mercaptopropyltrimethoxysilane and chitosan coated magnetic nanoparticles have a lower tendency to agglomerate and are much more stable than bare magnetic nanoparticles.[26]

STEM analysis

The surface morphology of synthesized Fe_3O_4 nanoparticles and chitosan coated magnetic nanoparticles is shown in Figure 8. Pure Fe_3O_4 particles have a spherical appearance. The images also reveal a slight tendency to aggregate due to the magnetic dipole moment between particles. The size measurements taken from STEM images are around ~ 15 nm. After coating with chitosan, the shape of the material obtained is also spherical. STEM images reveal that the shape of the nanoparticles did not change significantly because of the modification process.

Thermal analysis

The thermal stability of all the samples was examined by TGA and thermograms are given in Figure 9. For Fe_3O_4, dissociation corresponds to the loss of adsorbed water molecules at 150 °C.[33] Apart from this, there was no significant change in the TGA curve at 150-700 °C. This showed that Fe_3O_4 magnetic nanoparticles have excellent thermal stability, with about 96.6% residual mass. When looking at the TGA curve of magnetic nanoparticles modified with thiol end groups, a weight loss up to 100 °C and above 150 °C was observed due to the separation of the water molecules physically adsorbed on the surface and the removal of silanol groups.[34] When looking at the remaining mass at 750 °C, it was measured as 93.1%.

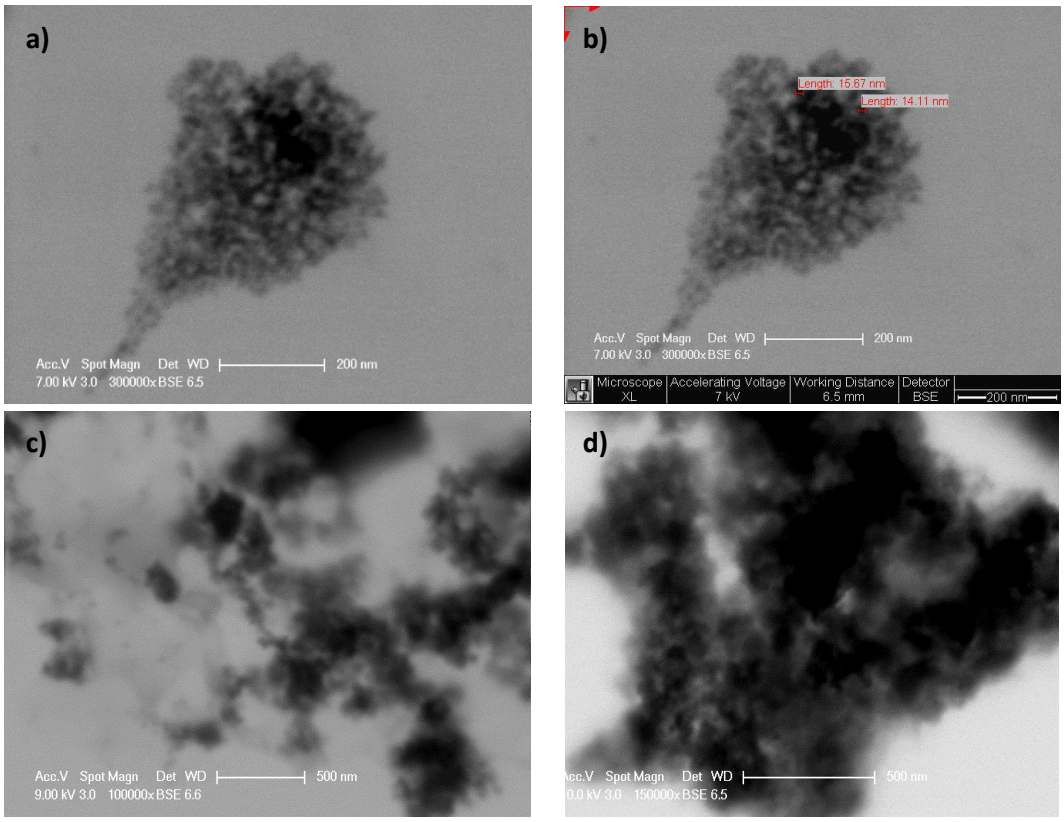

Figure 8: STEM images a) Fe_3O_4 nanoparticles 300.000X, b) Fe_3O_4 nanoparticles 300.000X, c) chitosan coated magnetic nanoparticles 100.000X and d) chitosan coated magnetic nanoparticles 100.000X

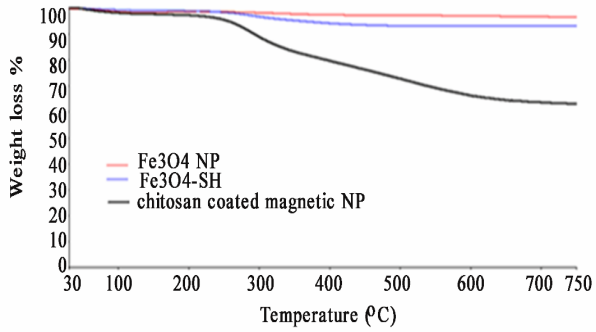

Figure 9: TGA thermograms of Fe_3O_4, Fe_3O_4-SH and chitosan coated magnetic nanoparticles

Compared with Fe_3O_4 magnetic nanoparticles, it is seen that the difference is due to the modification of the surface with 3-mercaptopropyltrimethoxysilane. Looking at the chitosan coated magnetic nanoparticles, the initial weight loss below 180 °C is due to water absorbed on the nanoparticles. The weight loss that occurs between 200-315 °C is related to the oxidation of the amino and hydroxyl groups of the polymer. Deacetylation of acid groups formed by the oxidation of OH groups before between 315-500 °C, as encountered later in the literature, is related to the release of nitrous oxides due to the loss of pre-oxidized amines and the breakdown of glycosidic bonds.[35-37] Finally, a weight loss between 500 and 700 °C occurs due to decomposition of the polymer chain. On the other hand, the weight loss of the chitosan coated magnetic nanoparticles at 750 °C was 37%, which is equivalent to a 33.6% (37-3.4) coating of the chitosan layer.

Drug loading and release

Encapsulation efficiency (EE, %) and drug loading content (DL, %) were calculated according to the equations specified in the corresponding section from the experimental part. The DL and EE results for each drug are shown in Table 2. According to the results, the DL and EE values of PTX were found to be higher than those of DOX. The two drugs are different in terms of their water solubility, and this may have affected the interaction of the nanoparticles with the drugs. PTX, a hydrophobic drug, can be interpreted as spontaneously and reversibly organizing into chitosan-Fe_3O_4 nanoparticles through non-covalent interactions. DOX, a hydrophilic drug, can be diffused between chitosan-Fe_3O_4 nanoparticles and localized in cavities.

The release profiles of DOX and PTX from the chitosan-Fe_3O_4 nanoparticles were measured in an aqueous solution of phosphate buffer solution at pH 7.4 and 5.0 (Figs. 10 and 11). The same process was done by loading DOX and PTX together. In general, it is seen that the drugs from the chitosan-Fe_3O_4 nanoparticles surface at both pH values are released in the first 6 hours and then the release slows down. This first rapid release, described as the "burst effect", occurs by drug desorption localized on the surface of the nanoparticles. At pH 7.4, 23.3% of the loaded DOX was released in 48 hours, while at pH 5, there was 30.5% release.

Also, the drug release from chitosan-Fe_3O_4 nanoparticles loaded with both DOX and PTX drugs together was investigated, and after 48 hours, doxorubicin release was determined as 27.16% at pH 5 and 22.48% at pH 7.4 (Figs. 12 and 13).

Paclitaxel was found to be released from PTX-loaded chitosan-Fe_3O_4 nanoparticles at a rate of 72.66% at pH 5 and of 41.45% at pH 7.4 after 48 hours. PTX release was determined as 62.15% at pH 5 and 50% at pH 7.4 after 48 hours from chitosan-Fe_3O_4 nanoparticles loaded with DOX and PTX drugs together. In general, drug release was higher at acidic pH. It is well known that the normal pH level in the human body is about 7.4, while near a cancerous tumor, it is about 5-5.5. In addition, more drug release at acidic pH may be protonation of amine groups of chitosan chains, electrostatic repulsion between chitosan chains, relaxation of nanoparticle structure, and increased drug release.

Table 2
Encapsulation efficiency (EE, %) and drug loading content (DL, %) results for DOX and PTX in chitosan-Fe_3O_4 nanoparticles and chitosan-Fe_3O_4 nanoparticles, loaded separately or together (mean ± SD)

Samples	DL (%)	EE (%)
DOX	2.552±0.0174	85.05±0.5508
PTX	2.877±0.0157	95.90±0.5237
(DOX+PTX)DOX	2.532±0.0136	84.40±0.4553
(DOX+PTX)PTX	2.747±0.0191	91.56±0.6361

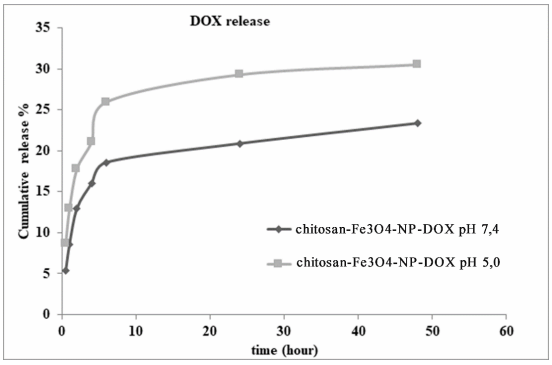

Figure 10: DOX release profile of chitosan-Fe_3O_4 nanoparticles formulations. Each data point represents mean ± SD of six measurements

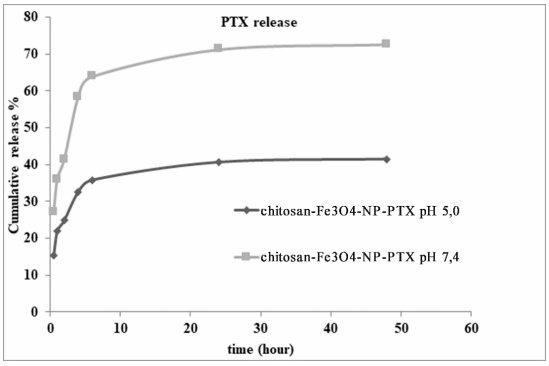

Figure 11: PTX release profile of chitosan-Fe_3O_4 nanoparticles formulations. Each data point represents mean ± SD of six measurements

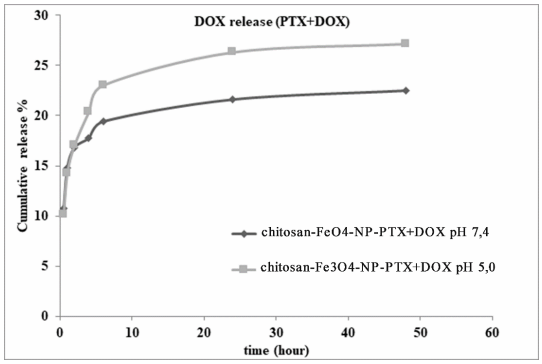

Figure 12: (DOX+PTX) DOX release profile of chitosan-Fe_3O_4 nanoparticles formulations. Each data point represents mean ± SD of six measurements

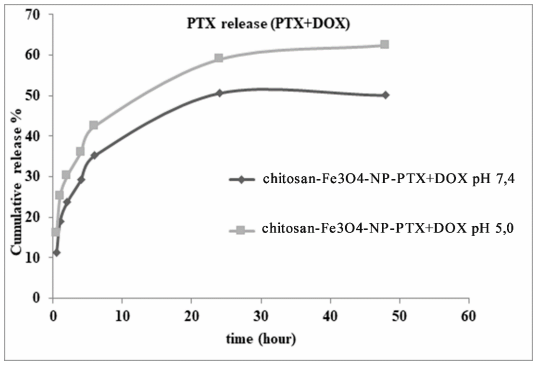

Figure 13: (DOX+PTX) PTX release profile of chitosan-Fe_3O_4 nanoparticles formulations. Each data point represents mean ± SD of six measurements

CONCLUSION

In summary, we have successfully synthesized a magnetically recoverable release system for cancer drugs DOX and PTX. The ATR-FTIR results proved the successful modification of magnetic nanoparticles with thiol end groups. ^{1}H-NMR and ATR-FTIR spectra were used to prove the successful modification of chitosan. Dimensional analysis of the obtained magnetic nanoparticles, magnetic nanoparticles modified with thiol groups, and chitosan coated magnetic nanoparticles was performed with DLS and their size and shape properties were investigated with STEM. Allyl groups modified chitosan was coated on the thiol end groups modified magnetic nanoparticles by the thiol-en click reaction with UV rays. The loading and release of cancer drugs DOX and PTX onto and from the obtained drug delivery systems were examined. The release profiles of DOX and PTX from the chitosan-Fe_3O_4 nanoparticles were measured in an aqueous phosphate buffer solution at pH 7.4 and 5.0. The two drugs are different in terms of their water solubility, and this suggests that the interaction of the drug delivery systems with the drugs is different. The water-insoluble PTX was effectively loaded into the chitosan-Fe_3O_4 nanoparticles and slowly released up to 72.66% at pH 5, and 41.45% at pH 7.4 after 48 hours. The water-soluble DOX was effectively loaded into chitosan-Fe_3O_4 nanoparticles and slowly released up to 30.5% at pH 5 and 23.3% at pH 7.4 after 48 hours. The encapsulation efficiency (EE, %) and drug loading (DL, %) studies performed with the two drugs loaded separately and together revealed that the release of PTX was 95.90% as the only drug loaded and 91.56% when loaded in combination (DOX+PTX). These results suggest the promising potential of chitosan-Fe_3O_4 nanoparticles as a stable magnetic delivery system, with dual therapeutic effects for the treatment of cancer.

ACKNOWLEDGMENTS: This work was supported by Marmara University, Commission of Scientific Research Project (M.Ü.BAPKO) under grant FEN-C-YLP-080519-0165.

REFERENCES

[1] B. Tian, Y. Liu and J. Liu, *Eur. Polym. J.*, **154**, 110533 (2021), https://doi.org/10.1016/j.eurpolymj.2021.110533

[2] F. X. Gu, R. Karnik, A. Z. Wang, F. Alexis, E. Levy-Nissenbaum *et al.*, *Nano Today*, **2**, 14 (2007), https://doi.org/10.1016/S1748-0132(07)70083-X

[3] Y. Chen, W. Zhang, Y. Huang, F. Gao, X. Sha *et al.*, *Int. J. Pharm.*, **488**, 44 (2015), https://doi.org/10.1016/j.ijpharm.2015.04.048

[4] H. Baabur-Cohen, L. I. Vossen, H. R. Kruger, A. Eldar-Boock, E. Yeini *et al.*, *J. Control Release*, **257**, 118 (2017), https://doi.org/10.1016/j.jconrel.2016.06.037

[5] J. Bai, Y. Zhang, L. Chen, H. Yan, C. Zhang *et al.*, *Mater. Sci. Eng. C.*, **92**, 338 (2018), https://doi.org/10.1016/j.msec.2018.06.062

[6] M. A. Abdel-Hakeem, O. M. Abdel-Haseb, S. E. Abdel-Ghany, E. Cevik and H. Sabit, *J. Drug Deliv. Sci. Technol.*, **55**, 101423 (2020), https://doi.org/10.1016/j.jddst.2019.101423

[7] A. Mendoza-Garcia and S. Sun, *Adv. Funct. Mater.*, **26**, 3809 (2016), https://doi.org/10.1002/adfm.201504172

[8] E. Kianfar, *J. Supercond. Nov. Magn.*, **34**, 1709 (2021), https://doi.org/10.1007/s10948-021-05932-9

[9] G. M. Ziarani, M. Malmir, N. Lashgari and A. Badieib, *RSC Adv.*, **9**, 25094 (2009), https://doi.org/10.1039/C9RA01589B

[10] H. Aslam, S. Shukrullah, M. Y. Naz, H. Fatima, S. Ullah *et al*., *Part. Part. Syst. Charact.*, **38**, 2100179 (2021), https://doi.org/10.1002/ppsc.202100179
[11] C. Han, N. Cai, V. Chan, M. Liu, X. Feng *et al*., *Colloids Surf. A Physicochem. Eng. Asp.*, **559**, 104 (2018), https://doi.org/10.1016/j.colsurfa.2018.09.012
[12] W. Wang, B. Zhao, X. Meng, P. She, P. Zhang *et al*., *J. Drug Deliv. Sci. Technol.*, **43**, 388 (2018), https://doi.org/10.1016/j.jddst.2017.11.007
[13] A. V. Samrot, T. C. Sean, T. Kudaiyappan, U. Bisyarah, A. Mirarmandi *et al*., *Int. J. Biol. Macromol.*, **165**, 3088 (2020), https://doi.org/10.1016/j.ijbiomac.2020.10.104
[14] F. S. Rezaei, F. Sharifianjazi, A. Esmaeilkhanian and E. Salehi, *Carbohyd. Polym.*, **273**, 118631 (2021), https://doi.org/10.1016/j.carbpol.2021.118631
[15] S. Rajput, C. U. Pittman and D. Mohan, *J. Colloid Interface Sci.*, **468**, 334 (2016), https://doi.org/10.1016/j.jcis.2015.12.008
[16] K. Zhang, W. Yang, Y. Liu, K. Zhang, Y. Chen *et al*., *J. Mol. Struct.*, **1220**, 128769 (2020), https://doi.org/10.1016/j.molstruc.2020.128769
[17] N. Illy, M. Robitzer, R. Auvergne, S. Caillol, G. David *et al*., *J. Polym. Sci. A: Polym. Chem.*, **52**, 39 (2013), https://doi.org/10.1002/pola.26967
[18] A. Geçer, N. Yıldız, A. Çalımlı and B. Turan, *Macromol. Res.*, **18**, 986 (2010), https://doi.org/10.1007/s13233-010-1004-0
[19] J.-L. Gong, X.-Y. Wang, G.-M. Zeng, L. Chen, J.-H. Deng *et al*., *Chem. Eng. J.*, **185-186**, 100 (2012), https://doi.org/10.1016/j.cej.2012.01.050
[20] R. Roto, Y. Yusran and A. Kuncaka, *Appl. Surf. Sci.*, **377**, 30 (2016), https://doi.org/10.1016/j.apsusc.2016.03.099
[21] S. Zhang, Y. Zhang, J. Liu, Q. Xu, H. Xiao *et al*., *Chem. Eng. J.*, **226**, 30 (2013), https://doi.org/10.1016/j.cej.2013.04.060
[22] D. V. Quang, J. E. Lee, J.-K. Kim, Y. N. Kim, G. N. Shao *et al*., *Powder Technol.*, **235**, 221 (2013), https://doi.org/10.1016/j.powtec.2012.10.015
[23] F. G. Pearson, R. H. Marchessault and C. Y. Liang, *J. Polym. Sci.*, **43**, 101 (1960), https://doi.org/10.1002/pol.1960.1204314109
[24] S. Wu, A. Sun, F. Zhai, J. Wang, W. Xu *et al*., *Mater. Lett.* **65**, 1882 (2011), https://doi.org/10.1016/j.matlet.2011.03.065
[25] T. A. ElBayoumi, V. P. Torchilin and V. Weissig, in "Liposomes: Methods and Protocols", edited by G. G. M. D'Souza, vol. 1: Pharmaceutical Nanocarriers, Springer, 2010
[26] A. Ali, H. Zafar, M. Zia, I. U. Haq, A. R. Phull *et al*., *Nanotechnol. Sci. Appl.*, **9**, 49 (2016), https://doi.org/10.2147/NSA.S99986
[27] Z. A. Alothman, *Materials*, **5**, 2874 (2012), https://doi.org/10.3390/ma5122874
[28] A. Ulu, S. A. A. Noma, S. Koytepe and B. Ates, *Artif. Cells Nanomed. Biotechnol.*, **46**, 1035 (2018), https://doi.org/10.1080/21691401.2018.1478422
[29] B. Rudolf, M. Salmain, A. Z. Wilczewska, A. Kubicka, I. Misztalewska *et al*., *Colloids Surf. A: Physicochem. Eng. Asp.*, **457**, 142 (2014), https://doi.org/10.1016/j.colsurfa.2014.05.056
[30] A. Z. Wilczewska, A. Kosińska, I. Misztalewska-Turkowicz, A. Kubicka, K. Niemirowicz-Laskowska *et al*., *Appl. Surf. Sci.*, **487**, 601 (2019), https://doi.org/10.1016/j.apsusc.2019.05.159
[31] S.-F. Shi, J.-F. Jia, X.-K. Guo, Y.-P. Zhao, D.-S. Chen *et al*., *Int. J. Nanomed.*, **7**, 5593 (2012), https://doi.org/10.2147/IJN.S34348
[32] Y. Ding, S. Z. Shen, H. Sun, K. Sun, F. Liu *et al*., *Mater. Sci. Eng. C*, **48**, 487 (2015), https://doi.org/10.1016/j.msec.2014.12.036
[33] S. Nagappan, H. M. Ha, S. S. Park, N.-J. Jo and C.-S. Ha, *RSC Adv.*, **7**, 19106 (2017), https://doi.org/10.1039/C7RA00159B
[34] N. Wang, N. Gao, S. Jiang, Q. Fang and E. Chen, *Compos. B Eng.*, **42**, 1571 (2011), https://doi.org/10.1016/j.compositesb.2011.04.012
[35] A. G. Pérez, E. González-Martínez, C. R. Díaz-Águila, D. A. González-Martínez, G. G. Ruiz *et al*., *Colloids Surf. A: Physicochem. Eng. Asp.*, **591**, 124500 (2020), https://doi.org/10.1016/j.colsurfa.2020.124500
[36] T. M. Freire, L. M. U. Dutra, D. C. Queiroz, N. M. P. S. Ricardo, K. Barreto *et al*., *Carbohyd. Polym.*, **151**, 760 (2016), https://doi.org/10.1016/j.carbpol.2016.05.095
[37] I. V. Pylypchuk, D. Kolodynska, M. Koziol and P. P. Gorbyk, *Nanoscale Res. Lett.*, **11**, 168 (2016), https://doi.org/10.1186/s11671-016-1363-3